

The assembly of protein subunits and cofactors in photosystem I

Wolfram Saenger*[†], Patrick Jordan* and Norbert Krauß[‡]

The recently determined crystal structures of photosystems I and II at 2.5 Å and 3.8 Å resolution, respectively, have improved the structural basis for understanding the processes of light trapping, exciton transfer and electron transfer occurring in the primary steps of oxygenic photosynthesis. Understanding the assembly of the 12 protein subunits and 128 cofactors in photosystem I allows us to study the possible functions of the individual players in this protein–cofactor complex.

Addresses

*Institut für Chemie/Kristallographie, Freie Universität Berlin, Takustrasse 6, D-14195 Berlin, Germany

[†]e-mail: saenger@chemie.fu-berlin.de

[‡]Institut für Biochemie, Universitätsklinikum Charité der Humboldt-Universität zu Berlin, Monbijoustrasse 2, D-10117 Berlin, Germany

Current Opinion in Structural Biology 2002, 12:244–254

0959-440X/02/\$ – see front matter

© 2002 Elsevier Science Ltd. All rights reserved.

Abbreviations

Chl <i>a</i>	chlorophyll <i>a</i>
EM	electron microscopy
EPR	electron paramagnetic resonance
ETC	electron transfer chain
Fd	ferredoxin
FNR	ferredoxin-NADP ⁺ oxidoreductase
LHCI	light-harvesting complex I
MGDG	monogalactosyldiglyceride
P680	primary electron donor of PSII
P700	primary electron donor of PSI
PG	phosphatidylglycerol
PS	photosystem
TMH	transmembrane α helix

Introduction

The main energy source for life on earth is the conversion of solar energy into chemical energy by oxygenic photosynthesis performed in plants, green algae and cyanobacteria. These organisms contain thylakoid membranes that harbor two large protein–cofactor complexes, photosystems I and II (PSI and PSII). The photosystems catalyze the initial and fundamental steps of oxygenic photosynthesis: they trap sunlight through extended antenna systems and use the energy to excite the primary electron donors (P700 at PSI and P680 at PSII), each releasing one electron per reaction cycle.

The released electrons are translocated across the thylakoid membrane along organic and inorganic cofactors, known as the electron transfer chains (ETCs). The ETCs of PSI and PSII are connected by a pool of plastoquinones, the cytochrome *b₆/f* complex and the soluble proteins cytochrome *c₆* or plastocyanin, and cooperate in series. In this process, water acts as electron donor to the oxidized P680 in PSII, and atmospheric oxygen evolves as a by-product (Figure 1). The electrons are finally transferred to

the stromal side of PSI and used to reduce NADP⁺ to NADPH, which is catalyzed by ferredoxin-NADP⁺ oxidoreductase (FNR) (Figure 1). The series of electron transfer reactions is coupled to the consumption of protons at the stromal side of the thylakoid membrane (cytoplasmatic in cyanobacteria) and to the release of protons at the luminal side of the membrane. The resulting difference in the electrochemical potential across the thylakoid membrane drives ATP synthetase (not shown in Figure 1). In subsequent dark reactions, ATP and NADPH are used to reduce CO₂ to carbohydrates.

The large superfamily of photosynthetic reaction centers can be divided into two classes characterized by the nature of their terminal electron acceptors: Fe–S clusters (type I) and quinones (type II) [1]. PSII and purple bacterial reaction centers (PbRCs) belong to type II, whereas PSI has a type I reaction center. Well-resolved structures of PbRCs [2] and the medium-resolution (3.8 Å) structure of PSII isolated from the thermophilic cyanobacterium *Synechococcus elongatus* [3[•]] have been published. The recently described 2.5 Å resolution structure of PSI isolated from the same cyanobacterium [4^{••},5[•]] is discussed here with respect to the assembly and possible functions of protein subunits and cofactors.

Composition of cyanobacterial photosystem I

The protein matrix of PSI consists of 12 subunits, illustrated in Figure 2 with their molecular masses, number of transmembrane α helices (TMHs) and cofactors of the ETC. The amino acid sequences were derived by gene sequencing for 11 of the PSI subunits of *S. elongatus* [6]. An additional subunit was fitted to the 2.5 Å resolution electron density map [4^{••},5[•]] that corresponds to subunit PsaX, which could not be traced on the gene level, but was only isolated from two thermophilic cyanobacteria.

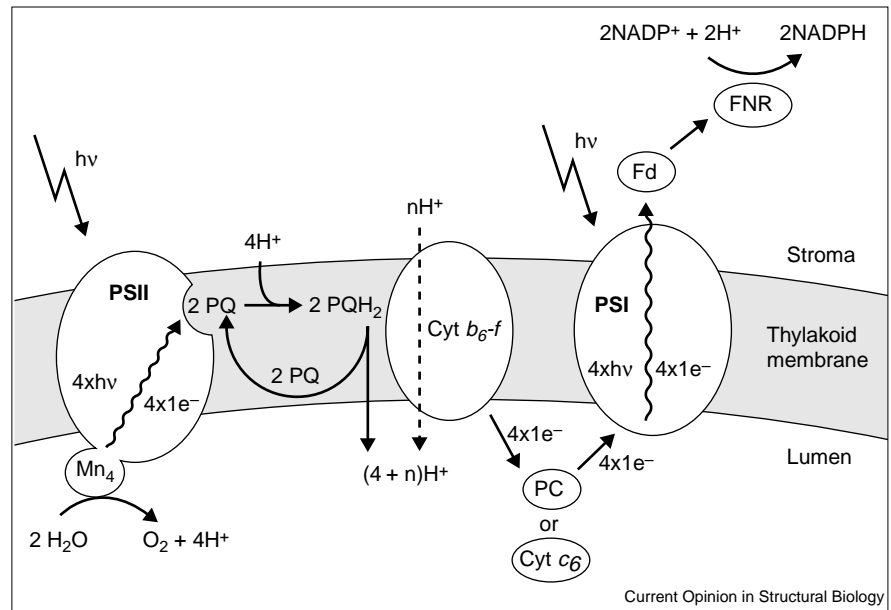
The number of cofactors bound to PSI is the largest found thus far in any protein–cofactor complex. In total, 128 cofactors are bound to PSI. They include 90 chlorophyll *a* (Chl *a*) in the antenna systems (see below) and five Chl *a*, one Chl *a*', two phylloquinones (vitamin K₁) and three Fe₄S₄ clusters that form the ETC. In addition, 22 carotenoids, four lipids and one putative Ca²⁺ were located in the 2.5 Å electron density map and 201 water molecules were identified [4^{••},5[•]].

Organization of protein subunits

Although higher plant and cyanobacterial PSIs are similar in structure and function, striking differences are found concerning their subunit composition, their association with peripheral antenna systems and their aggregation states (for reviews, see [7[•],8[•]]). In cyanobacteria, the phycobilisomes attached to the stromal surface of the thylakoid membrane

Figure 1

A schematic cut-through diagram of the thylakoid membrane, showing protein complexes (except ATP synthetase) engaged in the light reactions of oxygenic photosynthesis. At PSII, the light-driven ($h\nu$) reaction starts with oxidation of H_2O at the manganese cluster (Mn_4). The released electrons are translocated across the thylakoid membrane along the ETC involving plastoquinone (PQ), the cytochrome b_6/f complex (Cyt b_6-f) and plastocyanin (PC) or cytochrome c_6 (Cyt c_6). At PSI, the electrons are finally transferred to Fd on the stromal side of the membrane and terminate at FNR, which catalyzes the reduction of $NADP^+$ to NADPH. Stoichiometries of the reactions indicated refer to the production of a single molecule of O_2 .



can transfer excitation energy to the membrane-intrinsic core complexes of PSI and PSII, whereas in plants, light-harvesting protein-cofactor complexes are located in the thylakoid membrane and serve as peripheral antennae for both photosystems. Cyanobacterial PSI can be present as monomers and homotrimers [9,10]. The crystal structure shows that trimeric PSI from cyanobacteria resembles a cloverleaf (Figure 3a), with the monomers in the trimer being related by the C_3 axis of space group $P6_3$. It has been suggested that, in higher plants, trimeric PSI cannot be observed because the PSI core complex is almost completely surrounded by the light-harvesting complex LHCI [11]. Recent EM studies, however, show that LHCI binds only on one side of the PSI core complex and would not impede trimer formation [12**].

The two largest subunits of PSI, PsaA and PsaB, have a mass of about 83 kDa each and their primary structures are related, with 42% amino acid identity. Amino acids in these two subunits that bind ETC cofactors are almost strictly conserved, whereas amino acids that bind to antenna cofactors are only partially conserved. PsaA and PsaB feature 11 TMHs, each of which is connected by loops that are partially folded into smaller α helices and short β strands, as shown in the topography diagram for PsaA in Figure 4. PsaA and PsaB are located at the center of the PSI monomer and are related by a pseudo-twofold rotation axis (pseudo- C_2) (Figure 3a) [13].

Close (proximal) to the C_3 axis, the three TMHs of subunit PsaL interact with their symmetry-related mates and form

Figure 2

Schematic description of the subunit composition of cyanobacterial PSI. Under each subunit name (PsaA–PsaF, PsaL–M, PsaX), the number of TMHs within each subunit and the molar mass (kDa) of the subunit are indicated. Spectroscopically identified cofactors of the ETC are shown in red (P700, A_0 , A_1 , F_X , F_A , F_B). A_{cc} (green) denotes the ‘accessory’ Chl *a* determined in the X-ray study that escaped spectroscopic identification. *In addition to a single TMH, PsaF contains a kinked hydrophobic inner membrane α helix.

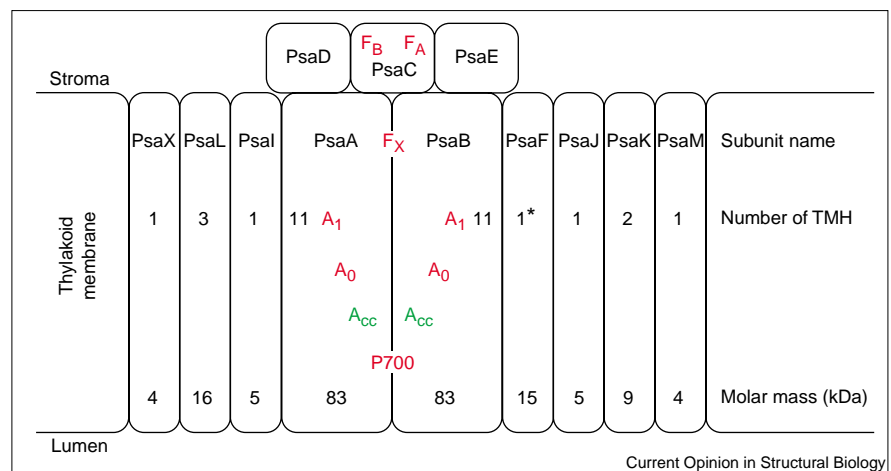
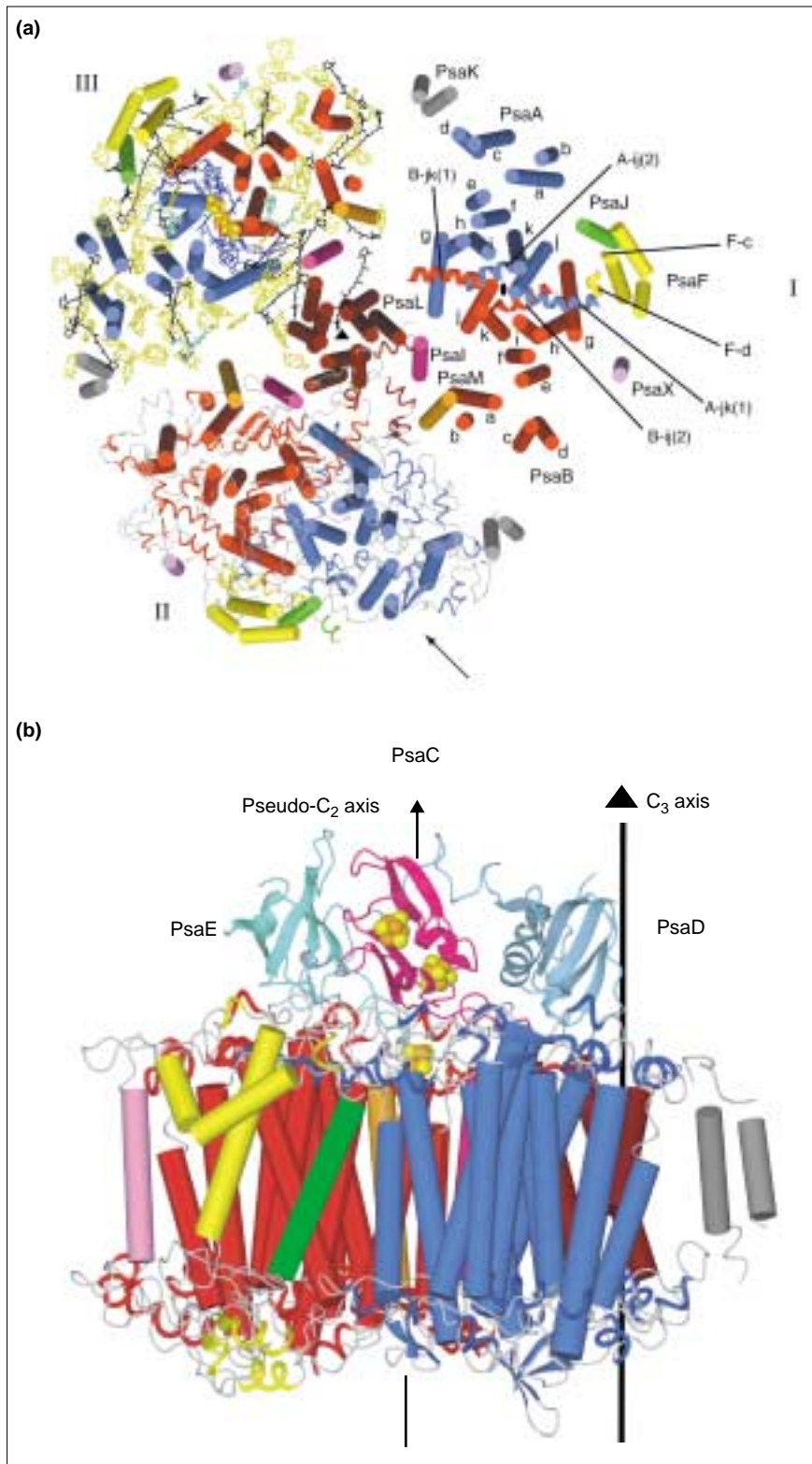


Figure 3

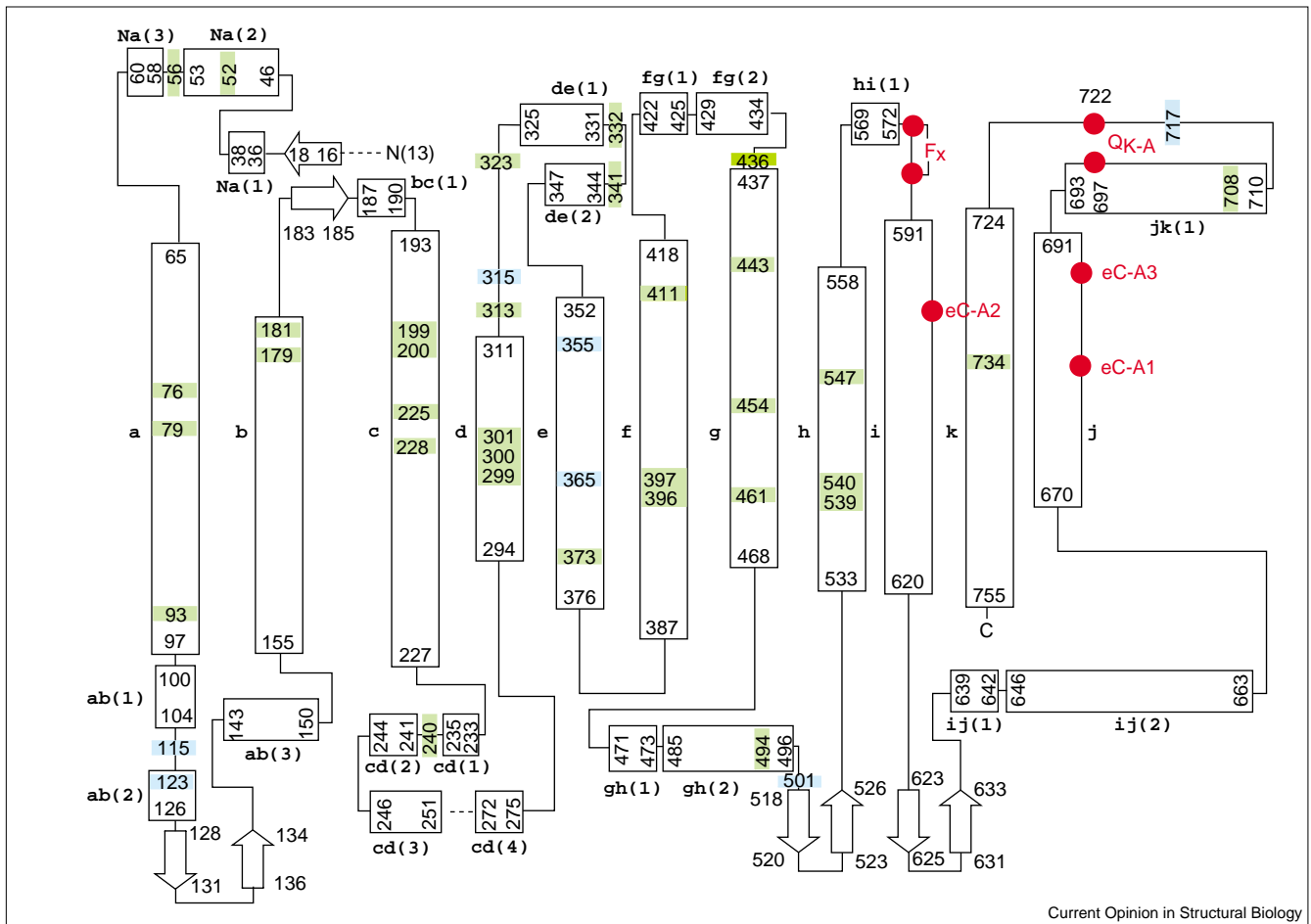


Three-dimensional structure of cyanobacterial PSI. (a) View along the membrane normal on the stromal side of PSI; subunits PsaC, PsaD and PsaE are omitted. The C_3 crystallographic symmetry axis is symbolized by \blacktriangle at the center of the trimer and the local pseudo- C_2 axis by a small, black ellipse at the center of monomer I between TMHs j belonging to PsaA (blue) and PsaB (red). In monomer I, TMHs are shown as cylinders and the α helices in loops A/B-jk (1), A/B-ij (2) and F-c, F-d are shown as spirals. For nomenclature, see Figure 4. Individual subunits are in different colors that are also used in monomers II and III. In monomer II, all secondary structure elements (TMH as cylinders; nontransmembrane α helices as spirals) and loops are shown. In monomer III, TMH are shown as cylinders and also indicated are the antenna Chl a (yellow), cofactors of the ETC (i.e. Chl a, Q_K -A, Q_K -B in blue), $[Fe_4S_4]$ clusters (orange/yellow), carotenoids (black) and lipids (cyan). (b) Side view of one PSI monomer, view direction indicated by the arrow at the bottom of (a). Color code as in (a). The C_3 axis is indicated by the black line to the right and the pseudo- C_2 axis by the vertical arrow. Figure reproduced from [4**] with permission.

the 'trimerization domain', augmented by subunit PsaI (featuring one TMH) and by the putative Ca^{2+} [4**]. On the other side of the PsaA–PsaB core and distal to the C_3 axis is subunit PsaF, with one TMH and an unusually

kinked hydrophobic inner membrane α helix, flanked by PsaJ and PsaX, with one TMH each. PsaK, with two TMHs, is located peripherally and close to the interface between the PSI monomers.

Figure 4



Topography of PsaA. α Helices are shown as rectangles and β strands as arrows. The 11 TMHs are denoted a–k and α helices in loops by two letters indicating the associated TMH followed by (1–4) describing the sequence of the α helices in the loops [e.g. ij(2) meaning the second α helix in the loop formed by TMHs i and j]. The N terminus is at N(13) (the first 12 amino acids could not be located) and the C terminus is at C. Amino acids directly or indirectly coordinating antenna cofactors are highlighted green for histidine and

blue for glutamine (115, 123, 355), threonine (501), tyrosine (315), isoleucine (717) and serine (365). Amino acids coordinating cofactors of the ETC (mentioned in the text) are indicated by red dots. For nomenclature of cofactors, see Figure 6. In the text, TMH and α helices are given by the subunit name (PsaA or short A) followed by the name of the TMH or α helix. β Strands are not named as they have only a structural role in stromal (top) and luminal (bottom) extramembrane loops.

The three stromal subunits, PsaC, PsaD and PsaE, do not feature TMHs and form a high ridge on the stromal side of the membrane (Figure 3b). PsaC is located on the pseudo- C_2 axis and wedged between PsaD and PsaE. The three subunits are arranged as a crescent surrounding part of the stromally exposed surface of PsaA, as had been proposed by Fromme *et al.* [14]. Lelong *et al.* [15] later verified this structure by EM analyses as the binding site of the electron carriers ferredoxin (Fd in Figure 1) or flavodoxin in cyanobacterial PSI. A different model, in which the Fd-binding site is located on top of the stromal ridge, was derived by EM of two-dimensional crystals of PSI from spinach [16^{*}]. As shown by the PSI crystal structure, PsaC is structurally similar to $2[Fe_4S_4]$ ferredoxins. In solution, however, the structure of PsaC from *Synechococcus* sp. PCC 7002 [17^{*}] differs significantly,

indicating that the folding of PsaC is modified during assembly into PSI. Besides PsaC, PsaD and PsaE are involved in the docking of Fd. PsaD plays a central role in the assembly of the stromal subunits, whereas PsaE may be required for cyclic electron transfer around PSI and for formation of the transient PSI–Fd–FNR complex [18] involved in NADP⁺ photoreduction (see [7^{*},8^{*},19^{*},20^{*}] for reviews on the stromal subunits).

Interactions between subunits

The TMHs of PSI are hydrophobic [6]. As hydrophobic interactions are largely determined by atom pairs at van der Waals distances and are considered weak and unspecific, they are not suited to define the well-organized assembly of subunits that is found in PSI. Consequently, each subunit is additionally engaged in specific hydrogen

Table 1

Hydrogen-bonding interactions between peripheral, membrane-intrinsic subunits involving mainchain (MC) and sidechain (SC) atoms in the PSI monomer [5*].

Subunit	MC–MC	MC–SC	SC–SC	Interacting subunits (number of interactions)
PsaF	1	2n, 6i	2i, 4s	PsaA(3), PsaB(7), PsaE(3), PsaF(1), PsaJ(1)
PsaI	2	2n, 3i	1i	PsaB(5), PsaL(2), PsaM(1)
PsaJ	3	2n	–	PsaF(5)
PsaK*	Only polyaniline model			
PsaL	3	4n, 2i	1s	PsaA(2), PsaB(5), PsaD(2), PsaL(1)
PsaM	–	3n, 3i	1i	PsaB(5), PsaL(2)
PsaX†	Ambiguous in some amino acids			
Total	9	27	9	

*Could only be modeled as polyaniline. †The amino acid sequence is questionable, as it has not been determined biochemically for *S. elongatus* PSI and has only been derived from the electron density. i, interaction with one partner charged; n, interaction between neutral partners; s, interaction with both partners charged (salt bridges).

bonds and salt bridges involving mainchain and sidechain atoms (a general overview is described in Table 1).

The large majority of the interactions between TMHs in PSI are of the type mainchain to sidechain, and many involve charged partners (i) (see Table 1). Interactions between mainchain atoms are primarily found in loop segments connecting the TMHs. Of the interactions between sidechains, many (six) are observed for PsaF (with four salt bridges), but only one each is observed for PsaI (i), PsaM (i) and PsaL (s). The interactions in the ‘trimerization domain’ are primarily of the mainchain to sidechain type.

The antenna chlorophyll *a*

The PSI core complex carries its own intrinsic ‘core’ antenna system to enlarge the absorption cross-section for sunlight over a wide spectral range so that efficient transfer of excitation energy to the primary electron donor P700 can occur. This process is related to transition dipole–dipole interactions between the involved donor and acceptor molecules that can be weakly or strongly coupled, depending on the distance between and relative orientation of these dipoles. In the PSI antenna system, weakly coupled Chl *a* dominate (Mg^{2+} – Mg^{2+} distances greater than 10 Å) and the energy transfer rates (k_{ET}) can be described by the Förster theory [21]. Of the 90 total core antenna Chl *a* of PSI, 79 are coordinated to PsaA–PsaB and 11 are bound to the peripheral subunits PsaJ (3 Chl *a*), PsaK (2), PsaL (3), PsaM (1) and PsaX (1) and to one phospholipid, phosphatidylglycerol (PG) (see below). The three stromal subunits (PsaC, PsaD and PsaE) and the membrane-intrinsic PsaI do not coordinate Chl *a*. The Mg^{2+} in the vast majority of

the antenna Chl *a* are axially coordinated by histidine (65 of the 90 total Chl *a*). The Mg^{2+} of the remaining antenna Chl *a* are axially coordinated by water (15) and sidechain oxygen atoms of glutamic acid (2), glutamine (3), aspartic acid, tyrosine, PG, peptide bond and one uncertain sidechain of PsaX (1 each). In all cases, the 15 water molecules bridge Mg^{2+} and an amino acid residue or a second water molecule [5*].

Most of the positions of Chl *a* coordinated by PsaA/PsaB follow roughly the pseudo- C_2 symmetry and can be divided into three groups (Figure 5a,b). The largest group contains 43 Chl *a* arranged in the form of an elliptically deformed cylinder bounded by TMHs PsaA/B a–d at the ‘outside’ and TMHs PsaA/B e–k at the ‘inside’ (for nomenclature, see Figure 4).

Two groups of 18 Chl *a* are located at the periphery of PsaA/PsaB. They are organized in two layers close to the stromal and luminal side of the membrane (Figure 5b). Another group, consisting of 11 Chl *a*, is coordinated by the peripheral subunits PsaJ, PsaX, PsaL and PsaM and the phospholipid PG (lipid III).

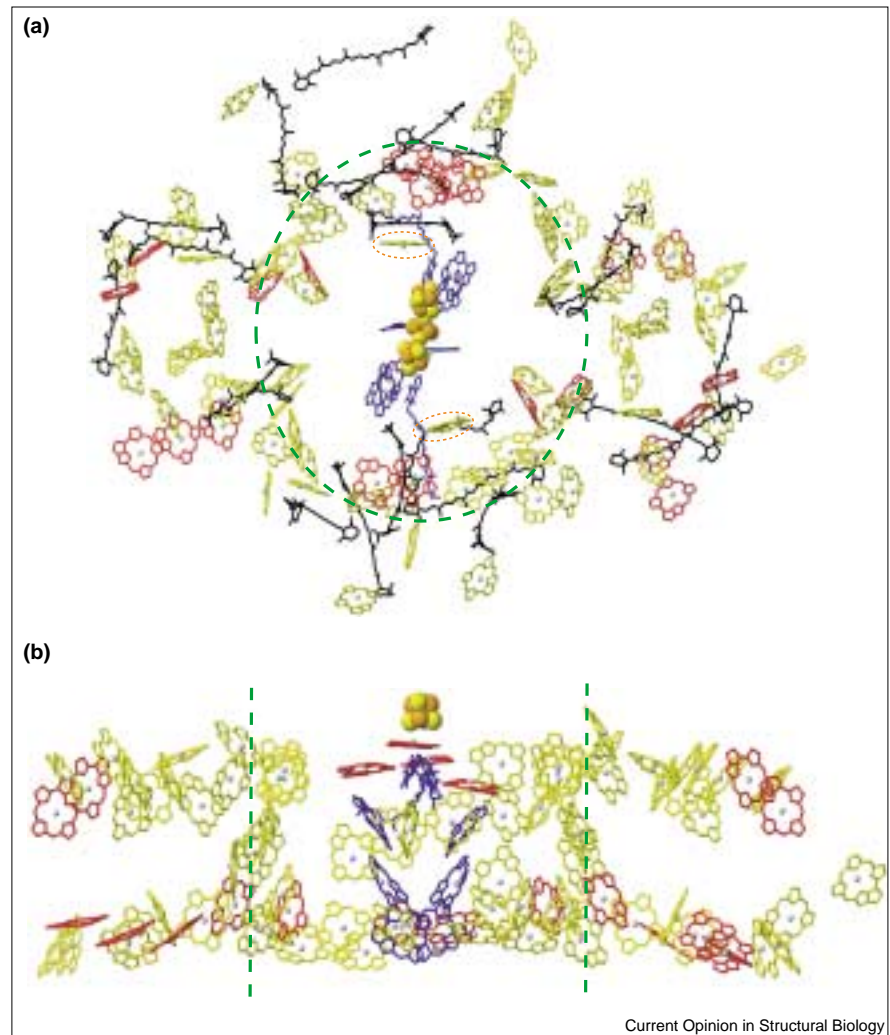
Two Chl *a*, aC-A40 and aC-B39, are special and are termed ‘connecting Chl *a*’ [13]. Of the entire antenna Chl *a*, these two are closest to the ETC and might serve as mediators of the excitation energy transfer from the antenna Chl *a* to the ETC (Figure 5a). According to kinetic modeling [22*,23*] based on the crystal structure of PSI at 4 Å resolution, the role of these Chl *a* in energy transfer is not as prominent as the structure might suggest.

Plant and cyanobacterial PSI core complexes are spectrally highly heterogeneous, with the major part of their core antenna, constituted by the ‘bulk’ Chl *a*, displaying a broad absorption band at 680 nm [23*]. In addition, they contain a few ‘red’ Chl *a* that absorb light at longer wavelengths than the ‘bulk’ Chl *a* and P700, corresponding to lower excitation energy. The biological significance of the ‘red’ Chl *a* in PSI is not fully understood, but they might enlarge the absorption cross-section for light energy in the red (long) wavelength region [24] or they might be required to focus the excitation energy in the vicinity of P700 [23*]. Spectroscopic data indicate close to 10 ‘red’ Chl *a* per P700 in trimeric PSI from *S. elongatus* [25]. The numbers and spectral properties of the ‘red’ Chl *a* strongly depend on the cyanobacterial or plant species [23*,26], whereas the properties of the ‘bulk’ Chl *a* most probably do not differ significantly among the PSI core complexes. A compartmental model containing a ‘bulk’ Chl *a* pool and one or two pools of ‘red’ Chl *a* was used to analyze time-resolved fluorescence data from various PSI core complexes [27**].

A red-shifted absorbance of Chl *a* can be caused by various factors [28], of which excitonic coupling of Chl *a* can be most safely deduced from the crystal structure. Applying

Figure 5

The excitonically coupled Chl *a* of the antenna system. The sidechains are omitted for clarity. (a) View along the membrane normal onto the stromal side. Color code as in Figure 3a. The 'red' Chl *a* dimers, which show the strongest coupling, and the Chl *a* trimer (lower left) are shown in red. The two 'connecting' Chl *a* forming the bridge between cofactors of the antenna and the ETC are marked by small ellipses (dotted orange). The large ellipse (dashed green) indicates the locus of the group of 48 Chl *a* mentioned in the text. (b) View along the membrane plane, rotated 90° with respect to (a). Fe₄S₄ clusters F_A and F_B are omitted. The vertical lines (dashed green) indicate the elliptical cylinder outlined in Figure 5a with dashed green line.



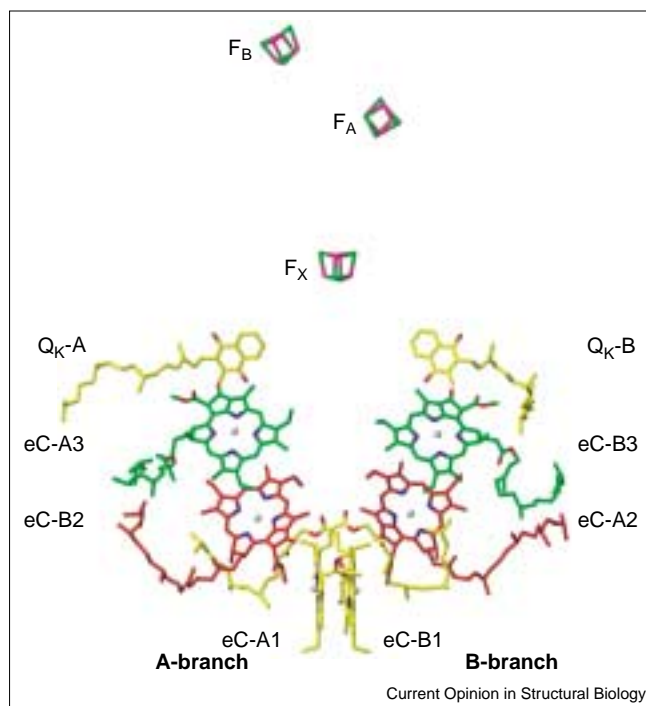
Current Opinion in Structural Biology

this criterion, possible candidates for the 'red' Chl *a* in *S. elongatus* PSI can be selected from the nine pairs of Chl *a* shown in Figure 5. In addition, there is an interesting Chl *a* trimer formed by stepwise arrangement of aC-B31, aC-B32 and aC-B33 (lower left in Figure 5). Only aC-B31 is coordinated to an amino acid, HisB470; the other two Chl *a* of the trimer are self-coordinated through water molecules. These pairs of Chl *a* and the trimer are characterized by very close center-to-center distances in the range 7.6–10.0 Å, and should be strongly coupled. The excitonic coupling of the Chl *a* colored red in Figure 5 alone, however, cannot explain the observed long-wavelength spectrum of PSI and suggests that other factors contribute also to this part of the spectrum. Spectroscopic studies on wild-type *Synechocystis* sp. PCC 6803 PSI, containing only four 'red' Chl *a*, and on its mutants deficient in PsaF, PsaK, PsaL and PsaM suggest that these four Chl *a* are bound to PsaA and/or PsaB, and are located close to the interfacial regions between PsaL and PsaM and the PsaA/B heterodimer [29*].

Carotenoids in photosystem I

Spectroscopic data have predicted 20 ± 4 carotenoids in the PSI monomer [30]. This is in agreement with the 22 carotenoids located in the crystal structure. They were modeled as β -carotenes, with 16 in all-*trans* conformation, five featuring one or two *cis* double bonds, and one as an incomplete molecule. This is consistent with biochemical data [31,32] indicating that β -carotene is the dominating carotenoid in PSI. The biological function of carotenoids in PSI is probably associated with the trapping of light energy and with the protection of the protein-cofactor complex and of the whole cell from photo-oxidative damage. Both functions rely on energy transfer processes according to the Dexter mechanism [33] that occur if chromophores are so close (at van der Waals distance) that their wave functions overlap. Energy transfer from the carotenoids to Chl *a* in the core complexes was found to be much more efficient in PSI than in PSII, suggesting that the major function of these cofactors in PSI is harvesting of light [34*], whereas it is photoprotection in PSII.

Figure 6



Cofactors of the ETC. The Chl *a* are denoted eC (for ETC Chl *a*), followed by coordinating subunit A (PsaA) or B (PsaB) and numbers 1–3 (1 for P700 [yellow], 2 for accessory Chl *a* [red] and 3 for A_0 [green]). A-branch and B-branch indicate cofactors predominantly coordinated to subunits PsaA and PsaB, respectively; however, note crossover occurs at eC-A2 and eC-B2. In P700, eC-A1 is Chl *a'* and eC-B1 is Chl *a*. Cofactors F_X , F_A and F_B are located near the stromal side of PSI and transfer the electron to the water-soluble electron carriers ferredoxin or flavodoxin (Fd in Figure 1), which convey it to FNR.

The carotenoids are deeply embedded in the membrane plane and only in a few cases are their head groups close to the stromal or luminal surface. They can be broadly grouped into six clusters [4^{••},5[•]] (not shown in Figure 5a), of which four (clusters 1–4) are associated with PsaA–PsaB and the other two clusters are additionally in contact with PsaF and PsaJ (cluster 5) and PsaI, PsaL and PsaM (cluster 6). The organization of the carotenoids in clusters 1, 2 and clusters 3, 4 are roughly related by the pseudo- C_2 axis, but this relation is less pronounced for clusters 5 and 6. The carotenoids are bound to the PSI complex by hydrophobic interactions with protein subunits and Chl *a*, and two are in close contact with the phytyl chains of the phylloquinones in the ETC.

Lipids in the photosystem I structure

The 2.5 Å resolution electron density of PSI shows four lipids: three PGs (I, III, IV) and one monogalactosyldiglyceride (MGDG, II). These lipids were also identified in PSI by immunological methods [32] (shown in monomer III, Figure 3a). PsaA binds to lipids I and III, and PsaB to lipids II and IV, and lipid IV is also in contact with PsaX. The positions of lipids I, II, and III, IV are

again related to each other by the pseudo- C_2 axis. Because lipids I and II are located close to the center of PSI and lipid III has an obvious function as it binds an antenna Chl *a*, the lipids must be considered as intrinsic components of PSI and not mere preparation artifacts [4^{••},5[•]].

The electron transfer chain

The heart of PSI is the ETC composed of 11 cofactors (Figures 2 and 6). The five Chl *a* and Chl *a'* and the two phylloquinones are arranged pairwise along the pseudo- C_2 axis between P700 and F_X , and follow the symmetry requirements. The two branches of cofactors are called A-branch and B-branch, depending on which protein, PsaA or PsaB, predominantly coordinates the cofactors. In both branches, there is a crossover at the 'accessory' Chl *a*, eC-A2 and eC-B2, [4^{••},5[•]] (for nomenclature, see Figure 6).

The key feature of the ETC is the primary electron donor P700, a heterodimer located close to the luminal side of PSI and formed by Chl *a* and its C13²-epimer Chl *a'* (as also suggested from biochemical data [35]), eC-B1 and eC-A1, respectively. Upon excitation, P700* releases an electron to form the positively charged radical P700⁺. Electron transfer proceeds toward the stromal side via one or both of the two branches of cofactors consisting of (1), the 'accessory' Chl *a* pair (eC-B2 and eC-A2; A_{cc} in Figure 2), which thus far have not been identified spectroscopically; (2) the pair of Chl *a* forming the primary electron acceptor A_0 (eC-A3 and eC-B3); (3) the pair of phylloquinones (vitamin K_1 ; Q_K -A and Q_K -B) forming the secondary acceptor A_1 ; (4) the Fe_4S_4 cluster (F_X) located virtually on the pseudo- C_2 axis [4^{••},5[•]] and near the stromal side of PSI. According to spectroscopic and kinetic data [36,37[•]], the electron continues by passing the Fe_4S_4 clusters F_A and F_B , which could be unambiguously assigned in the now available 2.5 Å electron density [4^{••},5[•]]. At F_B , the electron is transferred to the water-soluble electron carriers ferredoxin or flavodoxin (Fd in Figure 1), which convey it to FNR.

At the luminal side, P700 is shielded from solvent by α helices A/B-ij(2) (Figure 4) oriented almost parallel to the membrane plane. Mutations in the loop region B-ij [38] indicate that the hydrophobic surface formed by these α helices is an essential part of the docking site for cytochrome c_6 or plastocyanin (PC in Figure 1) when transferring an electron from PSII via the cytochrome b_6/f complex to PSI to re-reduce the oxidized P700⁺. The planes of the Chl *a'* and Chl *a* head groups are coordinated to HisA680 and HisB660, respectively, and oriented perpendicular to the membrane plane. They are parallel to each other at an interplanar distance of 3.6 Å and shifted laterally to yield a distance of 6.3 Å between Mg^{2+} cations. These data suggest that P700 is of (hetero)dimeric and not of monomeric character, as has been discussed controversially [39,40[•]], but the electron spin distribution in the radical cation P700⁺ is asymmetrical with a ratio of 85:15 on the two monomers (bound to PsaB:PsaA) [41[•]].

The hydrogen-bonding schemes between the protein matrix and the configurationally different Chl *a* and Chl *a'* of P700 are also different as three hydrogen bonds are formed with Chl *a'*, but none with Chl *a*. This inherent asymmetry is also reflected in the amino acids that interact with P700: none is conserved between PsaA and PsaB [4**,5*].

The head groups of the two 'accessory' Chl *a* (eC-B2 and eC-A2) are tilted by about 30° to the membrane plane. Their Mg²⁺ are coordinated by water molecules hydrogen bonded to AsnB591 and AsnA604, respectively. The head groups of the pair of candidates for the primary acceptor A₀ (eC-A3, eC-B3) are nearly parallel to those of the 'accessory' Chl *a* and feature a unique coordination with methionine sulfur, MetA688 and MetB668. According to the HSAB concept of hard and soft acids and bases, the interactions between the 'soft' base sulfur and the 'hard' acid Mg²⁺ should be weak, as also deduced from NMR studies on model compounds [42]. A still unanswered question is whether the weak axial ligand is responsible for the low redox potential (~-1.05 V [39]) of A₀. The phyloquinones Q_{K-A} and Q_{K-B}, of which one or both are identical to the secondary acceptor A₁, are in contact with the protein matrix by π-π stacking interactions to the conserved TrpA697 and TrpB677, respectively, in agreement with a model [43] proposed on the basis of the 4 Å resolution crystal structure [13]. In addition, hydrogen bonds are formed between the quinone oxygen atoms O4 (in *ortho* position to the phytol chain) and peptide NH of conserved LeuA722 and LeuB706, respectively. If the phyloquinone biosynthetic pathway is interrupted [44*], the phyloquinones in PSI can be replaced *in vivo* by plastoquinone-9, which supports forward electron transfer to F_X.

The Fe₄S₄ cluster F_X is coordinated by four cysteines in conserved loops A/B-hi: CysA574, CysA587, CysB565 and CysB574. This type of coordination of an Fe₄S₄ cluster is unique as it comprises two symmetry-equivalent and conserved segments belonging to two different subunits, PsaA and PsaB; in a comparable coordination, an Fe₄S₄ cluster [45] links two polypeptide chains in a homodimeric protein. The terminal clusters F_A and F_B are 12.3 Å apart and coordinated by the stromal subunit PsaC, the structure of which resembles bacterial 2[Fe₄S₄] ferredoxin, except for 25 additional amino acids in PsaC.

Does electron transfer use one or both branches of the electron transfer chain?

The existence of two branches of chemically equivalent organic cofactors (except for Chl *a* and Chl *a'* in P700) in the ETC raises an important question: are both branches or is only one branch (and which one) active in electron transfer? According to the Moser-Dutton approximation [46], the 'optimal' electron transfer rates are determined by the closest edge-to-edge distances between the cofactors. In the 2.5 Å resolution crystal structure of PSI, these distances are equivalent within the error limit (0.29 Å following Luzzati [47]), so this criterion cannot be used in the discussion.

The experimental and theoretical evidence for one or two branches is controversial [39,48*]. In a recent electron paramagnetic resonance (EPR) study involving PSI core complexes, in which the conserved tryptophans of the quinone-binding sites were mutated into phenylalanines, kinetic data are interpreted in favor of two active branches with slightly different kinetics for the transfer steps Q_{K-A} to F_X and Q_{K-B} to F_X [49**]. These data are supported by another EPR study [50] and FTIR difference spectra associated with the reduction of A₁ [51]. In our view, the large differences in the hydrogen bonding of Chl *a* and Chl *a'* in P700 suggest that one of the two branches may be favored in terms of the amplitude of electron transfer. Regarding the possibility of two different rates of electron transfer from Q_{K-A} or Q_{K-B} to F_X, there are some indications of asymmetry in the crystal structure: Q_{K-A} is 15 Å from the negatively charged PG (lipid I), whereas Q_{K-B} is at the same distance from the neutral MGDG (lipid II), and the local environments of Q_{K-A} and Q_{K-B} are not identical because different water networks are formed between these cofactors and F_X [4**,5*].

Conclusions: a PSI supercomplex and biogenesis of PSI and PSII

The crystal structure of PSI isolated from the thermophilic cyanobacterium *S. elongatus* is a solid basis for future spectroscopic, biochemical and molecular biological experiments designed to further our understanding of the function of the individual players in this protein-cofactor complex. Unfortunately, *S. elongatus* is a photoautotroph, so point mutations that interfere with the function of its PSI will reduce the growth rate and render physical methods difficult or even impossible because they require larger amounts of material. To circumvent this dilemma, a heterotrophic organism must be employed, but until now all attempts to crystallize PSI from other sources into X-ray-suitable form have been elusive.

A PSI supercomplex

Two recent papers describe the isolation of a PSI supercomplex from cyanobacteria grown under iron-deficient conditions [52**,53**], in which the additional protein IsiA is expressed. It is strongly homologous to subunit CP43 from PSII and is expected to harbor about 12 Chl *a*. On the basis of electron micrographs and the structures of PSI [13] and CP43 [3*], models were constructed in which the PSI trimer is surrounded by 18 IsiA molecules, yielding a supercomplex with a diameter of ~330 Å, a total molecular mass of 1 700 000 and featuring 504 antenna chlorophylls (3 × 96 PSI trimer plus 18 × 12 IsiA). Because in cyanobacteria grown under iron stress the PSI and light-harvesting phycobilisome content is likely to be reduced as not enough Fe₄S₄ clusters and biline chromophores can be formed, the large antenna of the supercomplex might compensate for this deficiency. The supercomplex compares with rings of light-harvesting proteins in anoxygenic purple bacteria. In addition to these and to the LHC trimers/dimers in chloroplasts, the IsiA rings are the third

known membrane-intrinsic peripheral chlorophyll-binding antenna. These systems are all structurally different but their assemblages show some similarities, suggesting convergent evolution [52**,53**].

Biogenesis of cyanobacterial PSI and PSII

A recent analysis of separated plasma and thylakoid membranes of the cyanobacterium *Synechocystis* sp. PCC 6803 [54**] showed that the former contain PSI proteins PsaA, PsaB, PsaC, PsaD and PSII proteins D1, D2, cytochrome b559 and chlorophyll. EPR spectra indicated that the subunits of PSI in the plasma membrane had assembled into a complex that was functionally active if illuminated by light and formed P700+. Concerning PSII, the essential protease CtpA, which cleaves the N terminus of precursor D1 protein to provide mature, functionally active D1, is tightly associated with the plasma membrane, but not with the thylakoid membrane. This led to a proposal for the biogenesis of PSI and PSII, suggesting that initially, reaction center cores, including cofactors, are assembled in the plasma membrane. They are then translocated to the thylakoid membrane and the addition of regulatory and light-harvesting subunits finally leads to complete PSI and PSII.

Acknowledgements

The work described here is a long-term collaboration with HT Witt and P Fromme, Technische Universität Berlin, and has been supported financially by DFG-Sonderforschungsbereiche 312 and 498, by Bundesministerium für Bildung und Forschung and by Fonds der Chemischen Industrie. We are grateful to Bernhard Loll for help with modifications of the figures.

References and recommended reading

Papers of particular interest, published within the annual period of review, have been highlighted as:

- of special interest
- of outstanding interest

1. Nitschke W, Rutherford AW: **Photosynthetic reaction centres: a variation of a common structural theme?** *Trends Biochem Sci* 1991, **16**:241-245.
2. Lancaster CRD, Bibikova MV, Sabatino P, Oesterhelt D, Michel H: **Structural basis of the drastically increased initial electron transfer rate in the reaction center from a *Rhodospseudomonas viridis* mutant described at 2.00 Å resolution.** *J Biol Chem* 2000, **275**:39364-39368.
3. Zouni A, Witt HT, Kern J, Krauß N, Saenger W, Orth P: **Crystal structure of photosystem II from *Synechococcus elongatus* at 3.8 Å resolution.** *Nature* 2001, **409**:739-743.
This paper describes the first crystal structure of a PSII with all cofactors essential for the electron transfer reactions in PSII and the majority of antenna Chl *a* located.
4. Jordan P, Fromme P, Witt HT, Klukas O, Saenger W, Krauß N: **Three dimensional structure of cyanobacterial photosystem I at 2.5 Å resolution.** *Nature* 2001, **411**:909-917.
The first structure of PSI at atomic detail is described, with all cofactors, including 22 carotenoids, four lipids, a Ca²⁺ cation and water molecules.
5. Jordan P: **Röntgenstrukturanalyse des trimeren Photosystem I aus dem Cyanobakterium *Synechococcus elongatus* bei 2.5 Å Auflösung [Ph.D. Thesis].** Berlin: Freie Universität; 2001. [Title translation: X-ray structural analysis of trimeric photosystem I from the cyanobacterium *Synechococcus elongatus* at 2.5 Å resolution.] PhD thesis (in German), providing many more details than given in [4**].
6. Mühlhoff U, Haehnel W, Witt HT, Herrmann RG: **Genes encoding eleven subunits of photosystem I from the thermophilic cyanobacterium *Synechococcus* sp.** *Gene* 1993, **127**:71-78.

7. Xu W, Tang X, Wang Y, Chitnis PR: **Proteins of the cyanobacterial photosystem I.** *Biochim Biophys Acta* 2001, **1507**:32-40.
A review of our current knowledge about the subunits of cyanobacterial PSI that are not involved in the binding of the cofactors of the ETC.
8. Scheller HV, Jensen PE, Haldrup A, Lunde C, Knoetzel J: **Role of subunits in eukaryotic photosystem I.** *Biochim Biophys Acta* 2001, **1507**:41-60.
A review on the functions of protein subunits in eukaryotic PSI. This review focuses on those features that are different from cyanobacterial PSI.
9. Westermann M, Neuschaefer-Rube O, Morschel E, Wehrmeyer W: **Trimeric photosystem I complexes exist *in vivo* in thylakoid membranes of the *Synechocystis* strain BO9201 and differ in absorption characteristics from monomeric photosystem I complexes.** *J Plant Physiol* 1999, **155**:24-33.
10. Kruij J, Chitnis PR, Lagoutte B, Rögner M, Boekema EJ: **Structural organization of the major subunits in cyanobacterial photosystem 1. Localization of subunits PsaC, -D, -E, -F, and -J.** *J Biol Chem* 1997, **272**:17061-17069.
11. Jansson S, Andersen B, Scheller HV: **Nearest-neighbor analysis of higher-plant photosystem I holocomplex.** *Plant Physiol* 1996, **112**:409-420.
12. Boekema EJ, Jensen PE, Schlodder E, van Breemen JFL, van Roon H, Scheller HV, Dekker JP: **Green plant photosystem I binds light-harvesting complex I on one side of the complex.** *Biochemistry* 2001, **40**:1029-1036.
A single-particle EM study on the supramolecular organization of PSI from spinach. LHCI, which provides the peripheral antenna of PSI in higher plants, is bound to the PSI core only on one side of the complex, close to PsaF and PsaJ.
13. Krauß N, Schubert W-D, Klukas O, Fromme P, Witt HT, Saenger W: **Photosystem I at 4 Å resolution represents the first structural model of a joint photosynthetic reaction and core antenna system.** *Nat Struct Biol* 1996, **3**:965-973.
14. Fromme P, Schubert W-D, Krauß N: **Structure of photosystem I. Docking sites for plastocyanin and ferredoxin, and the coordination of P700.** *Biochim Biophys Acta* 1994, **1187**:99-105.
15. Lelong C, Boekema EJ, Kruij J, Bottin H, Rögner M, Sétif P: **Characterization of a redox active crosslinked complex between cyanobacterial photosystem I and soluble ferredoxin.** *EMBO J* 1996, **15**:2160-2168.
16. Ruffe SV, Mustafa AO, Kitmitto A, Holzenburg A, Ford RC: **The location of the mobile electron carrier ferredoxin in vascular plant photosystem I.** *J Biol Chem* 2000, **275**:36250-36255.
An EM study on two-dimensional crystals of PSI from spinach cross-linked with Fd. The binding site of Fd deduced from difference Fourier maps is located on top of the stromal ridge, which is different from the docking site suggested for cyanobacterial PSI [14,15].
17. Antonkine ML, Liu G, Bentrop D, Bryant DA, Bertini I, Luchinat C, Golbeck JH, Stehlik D: **Solution structure of the unbound, oxidized photosystem I subunit PsaC, containing [4Fe-4S] clusters F_A and F_B: a conformational change occurs upon binding to photosystem I.** *J Biol Inorg Chem* 2002, in press.
This paper describes the three-dimensional NMR structure of the oxidized PsaC protein free in solution. Conformational differences between the solution structure and the structure of PsaC in the PSI complex [4**], which are most obvious in the N- and C-terminal regions with respect to the [Fe₄S₄]-binding core domain, are suggested to be associated with the assembly of the stromal subunits.
18. van Thor JJ, Geerlings TH, Matthijs HCP, Hellingwerf KJ: **Kinetic evidence for the PsaE-dependent transient ternary complex photosystem I/ferredoxin/ferredoxin:NADP+ reductase in a cyanobacterium.** *Biochemistry* 1999, **38**:12735-12746.
19. Sétif P: **Ferredoxin and flavodoxin reduction by photosystem I.** *Biochim Biophys Acta* 2001, **1507**:161-179.
A review on the electron transfer reactions between reduced PSI and the soluble proteins Fd and flavodoxin, including a detailed discussion of the functions of the stromal subunits PsaC, PsaD and PsaE.
20. Fromme P, Jordan P, Krauß N: **Structure of photosystem I.** *Biochim Biophys Acta* 2001, **1507**:5-31.
A review on the structure of PSI, relating the present knowledge from the crystal structure with functional studies on PSI.
21. Förster T: **Zwischenmolekulare Energiewanderung und Fluoreszenz.** *Ann Phys* 1948, **2**:55-75. [Title translation: Intermolecular energy transfer and fluorescence.]

22. Byrdin M, Rimke I, Schlodder E, Stehlik D, Roelofs T: **Decay kinetics and quantum yields of fluorescence in photosystem I from *Synechococcus elongatus* with P700 in the reduced and oxidized state: are the kinetics of excited state decay trap-limited or transfer-limited?** *Biophys J* 2000, **79**:992-1007.
- The excitation quenching efficiency of a cyanobacterial PSI core complex is shown to be different in the open (P700 reduced) and closed (P700 oxidized) states. The distance of the most red-shifted antenna Chl *a* to P700 is estimated to be ~35 Å and a structural/spectral information based model of the excitation energy transfer and decay is presented.
23. Gobets B, van Grondelle R: **Energy transfer and trapping in photosystem I.** *Biochim Biophys Acta* 2001, **1507**:80-99.
- A review article on excitation energy transfer and trapping processes in PSI.
24. Trissl H-W: **Long-wavelength absorbing antenna pigments and heterogeneous absorption bands concentrate excitons and increase absorption cross section.** *Photosynth Res* 1993, **35**:247-263.
25. Pålsson L-O, Flemming C, Gobets B, Van Grondelle R, Dekker JP, Schlodder E: **Energy transfer and charge separation in photosystem I: P700 oxidation upon selective excitation of the long-wavelength antenna chlorophylls of *Synechococcus elongatus*.** *Biophys J* 1998, **74**:2611-2622.
26. Karapetyan NV, Holzwarth AR, Rögner M: **The photosystem I trimer of cyanobacteria: molecular organization, excitation dynamics and physiological significance.** *FEBS Lett* 1999, **460**:395-400.
27. Gobets B, van Stokkum IHM, Rögner M, Kruij J, Schlodder E, Karapetyan NV, Dekker P, van Grondelle R: **Time-resolved fluorescence emission measurements of photosystem I particles of various cyanobacteria: a unified compartmental model.** *Biophys J* 2001, **81**:407-424.
- Analysis of room temperature time-resolved fluorescence data of monomeric and trimeric PSI core complexes from three different cyanobacteria. A simple compartmental model containing a chlorophyll pool absorbing at 702 nm and emitting at 712 nm as a common feature of all the complexes reproduces the kinetic data.
28. Fleming GR, van Grondelle R: **Femtosecond spectroscopy of photosynthetic light-harvesting systems.** *Curr Opin Struct Biol* 1997, **7**:738-748.
29. Rätsep M, Johnson TW, Chitnis PR, Small GJ: **The red-absorbing chlorophyll a antenna states of photosystem I: a hole-burning study of *Synechocystis* sp. PCC 6803 and its mutants.** *J Phys Chem B* 2000, **104**:836-847.
- Spectroscopic investigations on wild-type cyanobacterial PSI in trimeric and monomeric forms, and mutants deficient in subunits PsaF, PsaK, PsaL and PsaM. Four chlorophylls are suggested to contribute to the 'red' absorption band at 708 nm and are assigned to two low energy states at ~708 nm and 714 nm. They are not bound to one of the small PSI subunits and are likely to be bound to PsaA and/or PsaB and located close to the interface between PsaL, PsaB and the PsaA/PsaB core.
30. Flemming C: **Charakterisierung der Antennensysteme von monomeren und trimeren Photosystem I Komplexen.** Diplomarbeit, Technische Universität Berlin, 1996. [AU: Is this a book? Please provide a translation for the title.]
31. Coufal J, Hladik J, Sofrova D: **The carotenoid content of photosystem 1-pigment-protein complexes of the cyanobacterium *Synechococcus elongatus*.** *Photosynthetica* 1989, **23**:603-616.
32. Makewicz A, Radunz A, Schmid GH: **Comparative immunological detection of lipids and carotenoids on peptides of photosystem I from higher plants and cyanobacteria.** *Z Naturforsch (Sect C)* 1996, **51**:319-328.
33. Dexter D: **A theory of sensitized luminescence in solids.** *J Chem Phys* 1953, **21**:836-850.
34. Kennis JTM, Gobets B, van Stokkum IHM, Dekker JP, van Grondelle R, Fleming GR: **Light harvesting by chlorophylls and carotenoids in the photosystem I core complex of *Synechococcus elongatus*: a fluorescence upconversion study.** *J Phys Chem* 2001, **105**:4485-4494.
- The kinetics and efficiencies of energy transfer and trapping processes in PSI is studied analyzing time-resolved emission of light by the fluorescence upconversion technique. Energy transfer from carotenoids to chlorophylls is shown to occur from two different excited states of the carotenoids, the overall yield being ~90%.
35. Maeda H, Watanabe T, Kobayashi M, Ikegami I: **Presence of two chlorophyll *a*' molecules at the core of photosystem I.** *Biochim Biophys Acta* 1992, **1099**:74-80.
36. Golbeck JH: **A comparative analysis of the spin state distribution of *in vitro* and *in vivo* mutants of PsaC.** *Photosynth Res* 1999, **61**:107-144.
37. Shinkarev VP, Vassiliev IR, Golbeck JH: **A kinetic assessment of the sequence of electron transfer from F_X to F_A and further to F_B in photosystem I: the value of the equilibrium constant between F_X and F_A .** *Biophys J* 2000, **78**:363-372.
- Kinetic analysis of dark relaxation of P700⁺ in preparations of intact PSI and of PSI devoid of F_A and of both F_A and F_B indicates F_A to be the electron acceptor proximal to F_X . The equilibrium constant for electron transfer from F_X to F_A is estimated to be ~47 at room temperature.
38. Sun J, Xu W, Hervás M, Navarro JA, De La Rosa MA, Chitnis PR: **Oxidizing side of the cyanobacterial photosystem I. Evidence for interaction between the electron donor proteins and a luminal surface helix of the PsaB subunit.** *J Biol Chem* 1999, **274**:19048-19054.
39. Brettel K: **Electron transfer and arrangement of the redox cofactors in photosystem I.** *Biochim Biophys Acta* 1997, **1318**:322-373.
40. Webber AN, Lubitz W: **P700: the primary electron donor in photosystem I.** *Biochim Biophys Acta* 2001, **1507**:61-79.
- A review on the primary electron donor of PSI, with a focus on its electronic structure as determined by optical spectroscopy and magnetic resonance techniques.
41. Káb H, Fromme P, Witt HT, Lubitz W: **Orientation and electronic structure of the primary donor radical cation P700⁺ in photosystem I: a single crystal EPR and ENDOR study.** *J Phys Chem* 2001, **105**:1225-1239.
- EPR and ENDOR spectroscopic study on the orientation, structure and spin distribution of P700⁺ using single crystals of PSI.
42. Boxer SG, Bucks RR: **Chlorophyll-amino acid interactions in synthetic models.** *Isr J Chem* 1981, **21**:259-264.
43. Kamlowski A, Altenbach-Greulich B, van der Est A, Zech SG, Bittl R, Fromme P, Lubitz W, Stehlik D: **The quinone acceptor A_1 in photosystem I: binding site, and comparison to Q_A in purple bacteria reaction centers.** *J Phys Chem* 1998, **102**:8278-8287.
44. Zybailov B, van der Est A, Zech SG, Teutloff C, Johnson TW, Shen G, Bittl R, Stehlik D, Chitnis PR, Golbeck JH: **Recruitment of a foreign quinone into the A_1 site of photosystem I. II. Structural and functional characterization of phyloquinone biosynthetic pathway mutants by electron paramagnetic resonance and electron-nuclear double resonance spectroscopy.** *J Biol Chem* 2000, **275**:8531-8539.
- One out of a series of papers from the same authors describing studies on PSI isolated from cyanobacterial mutants, in which biosynthesis of the native electron acceptor phyloquinone is interrupted. In the mutant studied in this paper by EPR and ENDOR spectroscopy, plastoquinone-9 occupies the A_1 site in an orientation similar to the native electron acceptor, and is functionally active in accepting an electron from A_0^- and passing the electron forward to the iron-sulfur clusters.
45. Locher KP, Hans M, Yeh AP, Schmid B, Buckel W, Rees DC: **Crystal structure of the *Acidaminococcus fermentans* 2-hydroxyglutaryl-CoA dehydratase component A.** *J Mol Biol* 2001, **307**:297-308.
46. Moser CC, Dutton PL: **Engineering protein structure for electron transfer function in photosynthetic reaction centers.** *Biochim Biophys Acta* 1992, **1101**:171-176.
47. Luzzati V: **Traitement statistique des erreurs dans la détermination des structures cristallines.** *Acta Crystallogr* 1952, **5**:802-610. [Title translation: Statistical treatment of errors in the determination of crystalline structures.]
48. Brettel K: **Electron transfer in photosystem I.** *Biochim Biophys Acta* 2001, **1507**:100-114.
- The most recent review article on electron transfer reactions in PSI.
49. Guergova-Kuras M, Boudreaux B, Joliot A, Joliot P, Redding K: **Evidence for two active branches for electron transfer in Photosystem I.** *Proc Natl Acad Sci USA* 2001, **98**:4437-4442.
- A recent discussion on the subject of whether there are one or two branches of electron transfer in PSI is backed up with spectroscopic and mutational studies on the transfer steps Q_K-A and $Q_K-B \rightarrow F_X$. The authors conclude that both the A- and the B-branch are active in electron transfer in PSI.

50. Muhiuddin IP, Heathcote P, Carter S, Purton S, Rigby SE, Evans MCW: Evidence from time resolved studies of the P700⁺/A₁⁻ radical pair for photosynthetic electron transfer on both the PsaA and PsaB branches of the photosystem I reaction centre. *FEBS Lett* 2001, 503:56-60.
51. Hastings G, Sivakumar V: A Fourier transform infrared absorption difference spectrum associated with the reduction of A₁ in photosystem I: are both phylloquinones involved in electron transfer? *Biochemistry* 2001, 40:3681-3689.
52. Bibby TS, Nield J, Barber J: Iron deficiency induces the formation of an antenna ring around trimeric photosystem I in cyanobacteria. *Nature* 2001, 412:743-745.

See annotation to [53**].

53. Boekema EJ, Hifney A, Yakushevskaya AE, Plotrowski M, Kestera W, Berry S, Michel K-P, Pistorius EK, Kruij J: A giant chlorophyll-protein complex induced by iron deficiency in cyanobacteria. *Nature* 2001, 412:745-748.

References [52**,53**] use EM and modeling to show the structure of a supercomplex formed between cyanobacterial PSI trimer and 18 IsiA molecules containing Chl *a*.

54. Zak E, Norling B, Maitra R, Huang F, Anderson B, Pakrasi HB: The initial steps of biogenesis of cyanobacterial photosystems occur in plasma membranes. *Proc Natl Acad Sci USA* 2001, 98:13443-13448.

The biogenesis of PSI and PSII in cyanobacteria is initiated by the assembly of core reaction centers containing chlorophyll in the plasma membrane, followed by translocation to the thylakoid membrane, where the remaining subunits are added.